American Journal of Civil Engineering
2025, Vol. 13, No. 3, pp. 122-136
https://doi.org/10.11648/j.ajce.20251303.12

Research Article

Comparative Case Study of RC Frame Using Finite Element Modeling Under NBC 105:2020 and IS 1893 (Part 1):2016

Pawan Dumre[1, *], Mahendra Acharya[2], Asim Timalsina[3], Ajay Yadav[4], Sunil Acharya[5], Bishal Dhakal[6], Manish Kumar Gautam[1], Prinesh Maharjan[1]

[1]Department of Civil Engineering, Khwopa Engineering College, Purbanchal University, Bhaktapur, Nepal
[2]Central Department Geology, Tribhuvan University, Kathmandu, Nepal
[3]Department of Geology, Tri-Chandra Multiple Campus, Tribhuvan University, Kathmandu, Nepal
[4]Department of Civil & Rural Engineering, Nepal Engineering College, Bhaktapur, Nepal
[5]Department of Civil Engineering, Lumbini Engineering College, Pokhara University, Rupandehi, Nepal
[6]Department of Civil Engineering, Kathmandu Engineering College, Tribhuvan University, Kathmandu, Nepal

Abstract

Nepal's high seismic vulnerability necessitates stringent design codes to mitigate infrastructure risks. This study compares a regular reinforced concrete frame under Nepal's NBC 105:2020 and India's IS 1893 (part 1):2016 using finite element modeling in ETABS and SAP2000 commercial software, incorporating stiffness modifiers prescribed in the codes. Seismic parameters are compared in both ETABS and SAP2000, and for design forces and reinforcement requirements, only ETABS is used. Seismic analyses employed Equivalent Static and Response Spectrum methods. Results reveal NBC 105:2020 mandates double the base shear compared to IS 1893:2016, with lateral displacements surging by 50.6–66.6% under static analysis and 106–108% under dynamic analysis. Drift patterns mirrored displacement trends, showing similar percentage increases. Double base shear, amplified lateral displacements and drifts, consistent across both software analysis approaches, underscore NBC 105:2020's heightened design forces and reinforcement demands, particularly in lower floors. For beams, NBC 105:2020 required 12.7% more reinforcement, 11.6% higher moments, 110% lower torsion while maintaining comparable shear forces. Columns under NBC exhibited 79.78% higher axial forces, Floor-wise fluctuation in biaxial moments and 10.6% more reinforcement, with lower floors disproportionately impacted. This study suggests that municipalities and engineers in Nepal to follow the NBC code. While NBC 105:2020's stricter seismic provisions—requiring more robust structural systems, amplified design forces, and higher reinforcement demands compared to IS 1893 (Part 1):2016—escalate construction costs, its conservative approach ensures enhanced seismic resilience, critical for high-seismic-risk regions like Nepal.

Keywords

NBC 105:2020, IS 1893 (Part 1):2016, Reinforced Concrete Frames, Finite Element Modeling, ETABS/ SAP2000

*Corresponding author: pawandumre10@gmail.com (Pawan Dumre)

Received: 4 May 2025; **Accepted:** 19 May 2025; **Published:** 20 June 2025

1. Introduction

Nepal ranks among the world's most disaster-prone nations, positioned 11th globally in seismic vulnerability [1]. Its geological setting—within the Nepal Himalaya's fold-thrust belt and imbricate fault systems [2]—is shaped by the ongoing subduction of the Indian Plate beneath the Eurasian Plate at 30–40 mm/year [3]. This tectonic interaction accumulates substantial strain energy, capable of generating megathrust earthquakes exceeding Mw 8.0 [4]. The abrupt release of this energy through seismic events poses catastrophic risks to infrastructure and human settlements, as evidenced by Nepal's devastating historical earthquakes. A comprehensive analysis by [5], Revisiting Major Historical Earthquakes in Nepal, highlights recurrent seismic devastation, including the 2015 Gorkha earthquake sequence (Mw 7.8 mainshock and Mw 7.2 aftershock), which caused 8,673 fatalities and economic losses equating to nearly half of Nepal's GDP (~USD 10 billion) at that time [6, 7].

In Nepal, over two-thirds of earthquake-induced casualties stem from the collapse of non-engineered or poorly constructed buildings [8]. Mitigating this risk necessitates stringent implementation of seismic-resistant design codes. Following the 2015 disaster, Nepal revised its National Building Code (NBC 105:2020), significantly elevating base shear requirements by 28.59% (Ultimate Limit State) and 22.74% (Serviceability Limit State) compared to its 1994 predecessor [9]. Despite this update, many municipalities persist in permitting the use of India's seismic code (IS 1893 (Part 1):2016), partly due to shared tectonic and geotechnical conditions along their contiguous borders [10].

Critical disparities exist between NBC 105:2020 and IS 1893:2016. These include divergent design spectra, base shear computation methodologies, and stiffness modifiers: NBC incorporates both flexural and shear stiffness modifiers, whereas IS 1893 considers only the former. Prior studies remain somewhat non-comprehensive in terms of evaluating the specific criteria (seismic parameters, design forces, and reinforcement requirements) used to approve any RC building—residential or commercial—in municipalities, and they also report contradictory findings. For instance, [11] identified higher seismic parameters in NBC 105:2020 but omitted comparative analyses of design forces and reinforcement. Conversely, [12] reported negligible differences in reinforcement quantities between NBC 105:2019 (not the most recently updated version) and IS 1893:2016, while [13] observed a 4.39% increase in reinforcement under NBC 105:2020—albeit without applying stiffness modifiers. A recent study [14] paradoxically found that IS 1893:2016 demands higher reinforcement than NBC 105:2020 and ASCE 7–16, but its reliance on a simplified Bare Frame model (excluding infill wall contributions) limits practical relevance. In Nepal, brick-infilled RC frames dominate construction practices, where infill walls critically influence lateral stiffness, mass distribution, and seismic performance.

This study conducts a rigorous comparative analysis of NBC 105:2020 and IS 1893:2016, incorporating property modifiers (flexural/shear stiffness) and full load considerations (dead, live loads, earthquake loads). Using ETABS (matches with manual calculations [15]) and SAP2000 (for validation of lateral displacement and drift), we evaluate discrepancies in seismic parameters, design forces, and reinforcement requirements. Our findings address a critical gap by providing a comparative analysis of two widely used reinforced concrete (RC) building codes in Nepal—NBC 105:2020 and IS 1893 (part 1):2016—while quantifying the economic implications of code selection. This work not only contrasts the seismic philosophies and structural outcomes of these codes but also provides actionable insights for Nepalese municipalities to optimize code adoption, balancing seismic safety and cost-effectiveness.

2. Methodology and Modelling Details

The study analyzed a seven-story regular reinforced concrete building in Kathmandu (plan dimensions: 27.254 × 24.0284 m; total height: 21 m, floor height 3m; Figures 1-2) using finite element models developed in ETABS and SAP2000. The concrete frame of the structure was designed per the Limit State Design philosophy of IS 456:2000 [16], with material properties, dead loads (IS 875 Part 1:1987), and live loads (IS 875 Part 2:1987) assigned as per Tables 1–2. Section sizes for beams, columns, and slabs were defined floor-wise (Table 3), and column bases were fully restrained to simulate fixed foundations. Earthquake loads were computed using both NBC 105:2020 [17] and IS 1893 (Part 1):2016 [18], with seismic mass derived from 100% dead load, 25% live load (≤3 kN/m²), and 50% live load (>3 kN/m²) to ensure accurate inertial force representation [19]. Rigid diaphragms were assigned to floors to replicate the in-plane stiffness of RC slabs [20], while slabs were discretized into a 4×4 mesh (16 quadrilateral elements) to balance computational efficiency and dynamic analysis precision [21]. Linear static (Equivalent Static Method) and dynamic (Response Spectrum Analysis) approaches were employed, with the latter favored for its enhanced accuracy in finite element frameworks [22]. ETABS served as the primary tool due to its validation with manual calculation [15], and SAP2000 was used for cross-validation to minimize software-specific biases. However, for design forces and reinforcement calculation only ETABS is used. Seismic parameters, design forces (beams/columns), and reinforcement demands were systematically compared to quantify code-driven discrepancies.

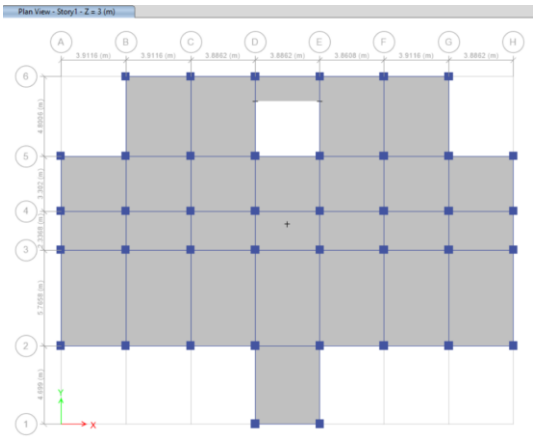

Figure 1. Plan of the building in ETABS.

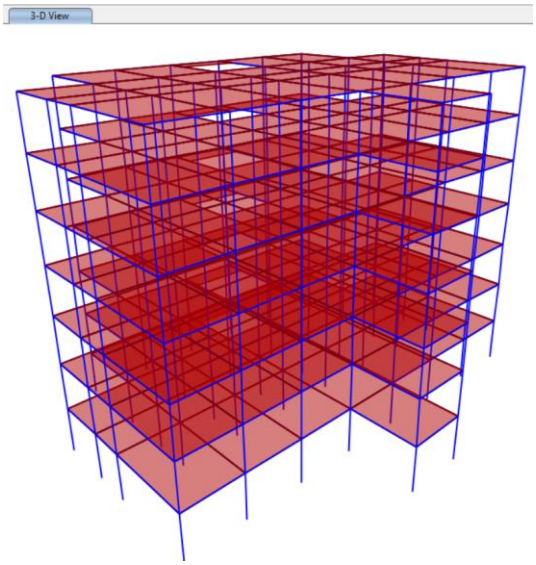

Figure 2. 3D FEM mathematical model in SAP2000.

Table 1. Material property using IS 1893 (Part 1): 2016 and NBC 105:2020 (ETABS and SAP2000).

Material	Property Value
Characteristic strength of concrete (fck)	25 MPa
Yield Strength of rebar (fy)	500 MPa
Specific unit weight of Brick Masonry (γ_b)	19 kN/m^3
Specific unit weight of reinforced concrete (γ_c)	25 kN/m^3

Table 2. Dead Loads and Live Loads using IS 1893 (Part 1): 2016 and NBC 105:2020 (ETABS and SAP2000).

SI. No	Loads	Weight
1	Live $\leq$ 3	2 kN/m^2
2	Live $>$ 3	3 kN/m^2
3	Roof Live	1.5 kN/m^2
4	Floor Finish	1.1 kN/m^2
5	Staircase	21 kN/m
6	Wall 9"	7.885 kN/m
7	Wall 4"	3.992 kN/m

Table 3. Size of the members using IS 1893 (Part 1): 2016 and NBC 105:2020 (ETABS and SAP2000).

Floor	Units	Beam	Column	Slab
1 to 4	mm	300 X 450	500 x 500	125
5 to 7	mm	300 X 450	400 X 400	125

3. Earthquake Loads

The seismic design frameworks of the Indian (IS 1893 (Part 1):2016 [18]) and Nepali (NBC 105:2020 [17]) codes diverge fundamentally in their hazard assessment methodologies. IS 1893 adopts a deterministic approach based on historical earthquake data, while NBC 105:2020 employs a probabilistic seismic hazard analysis (PSHA), defining peak ground acceleration (PGA) contours for a 475-year return period (10% probability of exceedance in 50 years). A critical advancement in NBC 105:2020 is the replacement of the outdated Performance Factor (K) [23] with modern response reduction factors: the ductility factor (Rμ) and over strength factor, (Ω), aligning with global seismic design philosophies that emphasize force reduction through ductility and structural resilience.

3.1. Elastic Site Spectra for Horizontal Loading in NBC105: 2020

Elastic site spectra design are normally estimated from the (PGA) proposed in seismic codes, for different general soil categories under free field soil conditions [24]. The Elastic site spectra for horizontal loading in ultimate state C (T) is determined using Eq. (1).

$$C\ (T)\ =\ C_h(T)\ Z\ I \tag{1}$$

Where, $C_h(T)$ is the Spectral Shape factor as per Eq. (3), Z is the Seismic Zoning factor and I is importance factor. The values of Z and I is specified in Table 4.

The elastic site spectra for Serviceability Limit State is be given by:

$$Cs\ (T)\ =\ 0.20\ C\ (T) \tag{2}$$

Where C (T) = elastic site spectra for horizontal loading determined from Eq. (1).

3.2. Spectral Shape Factor, $C_h(T)$

The Spectral Shape Factor is a value that adjusts how a structure responds to an earthquake, based on its frequency and vibration characteristics. Two different spectra are used for seismic coefficient method and modal response spectrum method in Nepali code. The spectral shape factor functions given in Figure 3 is used for Equivalent Static Method and those in Figure 4 is used for Modal Response Spectrum Method. Calculated by Eq. (3) using the parameters specified in Table 4.

$$Ch\ (T) = \begin{cases} 1 + (\alpha - 1) \times \frac{T}{Ta} & \text{if } T < Ta \\ \alpha & \text{if } Ta \leq T \leq Tc \\ \alpha\ [K + (1 - K)\ (\frac{Tc}{T})2]\ (\frac{Tc}{T})2 & \text{if } Tc \leq T \leq 6 \end{cases} \quad (3)$$

Where, Ch (T) is the Spectral Shape Factor for equivalent static method and response Spectrum Method, α is the peak spectral acceleration normalized by PGA, Ta and Tc are the lower and upper periods of the flat part of the spectrum, K is the coefficient that controls the descending branch of the spectrum and T is the fundamental time period.

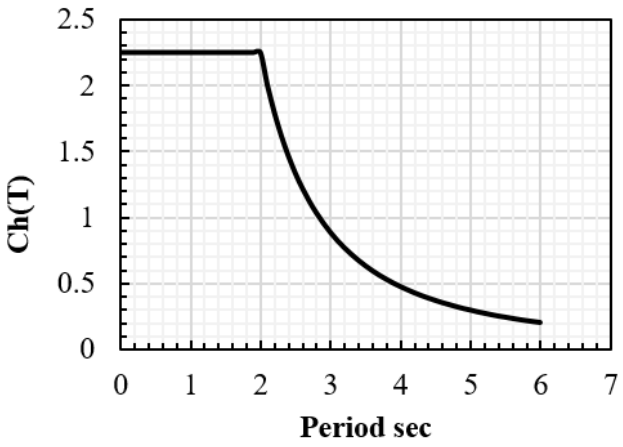

Figure 3. *Spectral Shape Factor, Ch(T) for equivalent Static Method soil type D.*

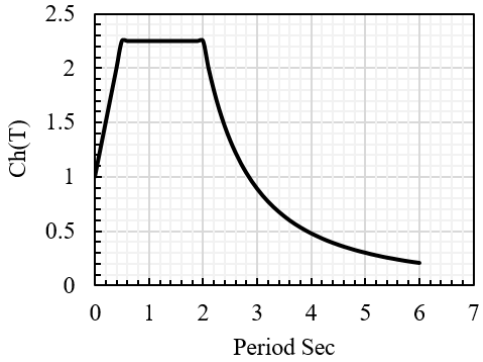

Figure 4. *Spectral Shape Factor, Ch(T) for Response Spectrum Method soil type D.*

3.3. Horizontal Base Shear Coefficient

For the ultimate limit state (ULS), the horizontal base shear coefficient (design coefficient), $C_{du,}$ is given by Eq. (4), and for the serviceability limit state (SLS), the horizontal base shear coefficient (design coefficient), Cds, is given by Eq. (5).

$$C_{du} = \frac{C(T)}{R\mu\ x\ \Omega u} \quad (4)$$

$$C_{ds} = \frac{Cs(T)}{\Omega s} \quad (5)$$

Where, C (T) is the elastic site spectra as per Eq. (1), Rμ is the ductility factor and **Ω**u and **Ω**s is the Over strength Factor for ULS and SLS, respectively refer to table 4 for values, Cs(T) is the elastic Site Spectra determined for serviceability limit state as per Eq. (2).

The fundamental period (*T*) was computed per NBC 105:2020 (Clauses 4.1.1 and 4.2) using the exponent K, which governs period-height scaling [25]. For response spectrum analysis, *Ch*(*T*) was manually calculated for Soil Type D (Figure 4) and input into ETABS and SAP2000. While IS 1893:2016 parameters (Table 5) are natively supported by both platforms, NBC 105:2020's dual-state framework necessitated manual adjustments to accommodate ULS/SLS distinctions. This underscores a key practical divergence: IS 1893 streamlines seismic load assignment, whereas NBC 105:2020 demands additional user intervention to replicate its nuanced requirements.

Table 4. *Calculation of seismic coefficients for equivalence static method and response spectrum method as per NBC: 105:2020 (ETABS and SAP2000).*

Inputs:	
Location of Building:	Kathmandu
Type of Structure:	Moment resisting concrete frame
Type of Building:	Reinforced Moment Resisting Frame

Inputs:		
Seismic Zoning Factor *(Table 4.5 NBC 105-2020)*	Z =	0.35
Importance Factor: (*Table 4.6 NBC 105-2020*)	I =	1
Height of Building:	h =	21
Soil Type for Kathmandu (*Refer table 4.4 NBC 105:2020*)	D	
Period of Vibration: (*Clause 5.1.2 NBC 105:2020*)		
For Reinforced Moment Resisting Frame	$T = 1.25x0.075xh^{0.75}$	0.92 Sec
Refer Table 4.1 NBC 105:2020		
Lower Period of the Flat Part of the Spectrum	Ta =	0
Upper Period of the Flat Part of the Spectrum	Tc =	2
Peak Spectral Acceleration Normalized by PGA	α =	2.25
Coefficient to control the descending branch of the Spectrum	K =	0.8
Note: The value of the flat spectrum Ta for response spectrum analysis is 0.5 second		
Refer Table 5.2 NBC 105:2020		
Ductility Factor for ULS State	Ru =	4
Overstrength Factor for ULS State	Ωu =	1.5
Overstrength Factor for SLS State	Ωs =	1.25
Calculation of Spectral Shape Factor: Ch (T) *(Clause 4.1.2 NBC 105:2020)*		
Since Ta<=T1<=Tc	Ch (T) =	2.250
Elastic Site Spectra for the Horizontal Loading *(Clause 4.1.1 NBC 105:2020)*	C(T) = Ch(T) Z I =	0.788
Elastic Site Spectra for the SLS State *(Clause 4.2 NBC 105:2020)*	Cs = 0.2 * C(T) =	0.158
Horizontal Base Shear Coefficient for Equivalent Static Method and response spectrum method		
Horizontal Base Shear Coefficient at the ULS State		
Cdu = C(T)/ (Ru x Ωu)	=	0.131
Horizontal Base Shear Coefficient at the SLS State		
Cds = Cs/ Ωs	=	0.126
Exponent related to the structural period *(Clause 4.2 NBC 105:2020)*	K =	1.210

Table 5. *Parameters required for assigning earthquake loads by equivalence static method and response spectrum methods as per IS 1893 (Part 1): 2016 (ETABS and SAP2000).*

Inputs	**Values**	**IS 1893 (Part 1): 2016**
Soil type	II	Table 4
Zone factor	0.36	Table 3, Zone 5
Importance factor	1	Table 8,
Response reduction factor	5	Table 9
Time Period	0.736	Clause 7.6.2
Damping ratio	0.05	Clause 7.2.4

4. Stiffness of Cracked Sections

The consideration of effective stiffness in elastic structural analyses is critical to mitigating displacement-induced damage and enhancing seismic performance under severe loading [26]. In reinforced concrete (RC) structures subjected to combined vertical and lateral loads, critical members experience flexural cracking near yield points, leading to progressive reductions in flexural stiffness (EI) as tensile zones degrade [27]. To address this, modern seismic codes prescribe property modifiers to simulate cracked section behavior. Both NBC 105:2020 and IS 1893:2016 specify identical flexural stiffness modifiers (Table 6), reducing EI to account for flexural cracking. While most of the seismic codes focus on effective flexural stiffness, a suitable shear stiffness modifier is also crucial for seismic design, this is especially the case when diagonal cracking occurs in heavily reinforced members [28]. Considering both modifiers fulfills the demands of ultimate limit state (ULS) and limit state of serviceability (SLS), the absence of effective shear stiffness modifiers in the Indian code contributes to discrepancies in analysis results.

Table 6. Stiffness Modifiers for Beams and Columns: NBC 105:2020 and IS 1893 (Part 1): 2016 (ETABS and SAP2000).

		NBC 105:2020		IS 1893: (Part 1) 2016	
SI no.	**Component**	**Flexural Stiffness**	**Shear Stiffness**	**Flexural Stiffness**	**Shear Stiffness**
1	Beam	0.35 Ec Ig	0.40 Ec Aw	0.35 Ec Ig	Not Specified
2	Columns	0.70 Ec Ig	0.40 Ec Aw	0.70 Ec Ig	Not Specified

In table 6, E_C is the elastic modulus of concrete, which is a measure of the material's ability to resist deformation under load. It defines the stiffness of the concrete material itself. Ig is the gross moment of inertia of the cross-section of a structural member (beam and column). It reflects the geometrical properties of the section and is calculated based on the full un-cracked cross-section of the member. A_w, is the effective shear area, depends on the type of structural member and its geometry.

5. Load Combinations

Load combinations are necessary to account for various potential scenarios that a structure may face, such as dead loads, live loads, and seismic forces. These combinations ensure that the structure is evaluated under different conditions to check its safety, stability, and serviceability. The Nepali code load combination is shown in Table 7, while the Indian code load combination is shown in Table 8.

Table 7. Load Combinations using NBC 105:2020 (ETABS and SAP2000).

SI. No	Combinations
1	1.2 DL + 1.5 LL
2	1.5 (DL + LL)
3	DL + 0.3 LL + EQx ULS
4	DL + 0.3 LL + EQy ULS
5	DL + 0.3 LL + RSx
6	DL + 0.3 LL - EQx ULS
7	DL + 0.3 LL - EQy ULS
8	DL + 0.3 LL - RSy

Abbreviations, DL = Dead Load, LL = Live Load, EQx ULS = Earthquake Load in the x-direction for ultimate limit state, EQy ULS = Earthquake Load in the y-direction for ultimate limit state, RSx = Response Spectrum Load in the x-direction, RSy = Response Spectrum Load in the y-direction.

Table 8. Load Combinations using IS 1893 (Part 1): 2016 (ETABS and SAP2000).

SI. No	Combinations
1	1.5 (DL + LL)
2	1.2 (DL + LL ± EQx)
3	1.2 (DL + LL ± EQy)
4	1.5 (DL ± EQx)
5	1.5 (DL ± EQy)
6	0.9 DL + 1.5 EQx
7	0.9 DL - 1.5 EQx
8	0.9 DL + 1.5 EQy

SI. No	Combinations
9	0.9 DL - 1.5 EQy
10	1.2 (DL + LL ± RSx)
11	1.2 (DL + LL ± RSy)
12	1.5 (DL ± RSx)
13	1.5 (DL ± RSy)
14	0.9 DL + 1.5 RSx or RSy

Abbreviations, DL = Dead Load, LL = Live Load, EQx = Earthquake Load in the x-direction, EQy = Earthquake Load in the y-direction, RSx = Response Spectrum Load in the x-direction, RSy = Response Spectrum Load in the y-direction.

6. Results and Discussion

6.1. Story Shear

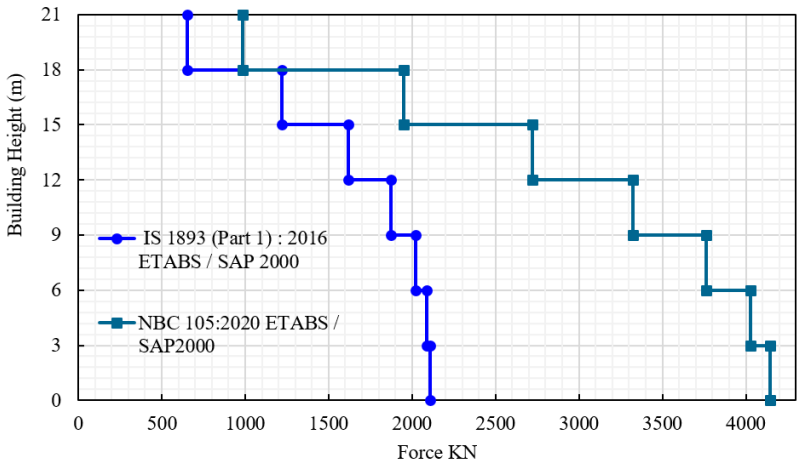

Figure 5. *Story shear as per IS 1893 (part 1):2016 and NBC 105:2020.*

As illustrated in Figure 5, story shear—the cumulative lateral force at each building level due to seismic loads—demonstrates a stark divergence between the Indian (IS 1893:2016) and Nepali (NBC 105:2020) codes. The NBC 105:2020-prescribed base shear (4145.73 kN at elevation 0 m) nearly doubles the IS 1893:2016 value (2106.06 kN), reflecting the Nepali code's conservative approach to seismic force estimation.

In symmetrical structures, shear distributions mirror each other in orthogonal directions due to balanced stiffness and mass distribution. However, asymmetrical configurations introduce torsional effects, leading to directional disparities in story shear demands. The elevated story shear forces under NBC 105:2020 necessitate robust structural systems, including enhanced reinforcement detailing and larger member sections, to accommodate greater energy dissipation demands.

6.2. Displacement and Inter-storey Drift

The displacement and inter-storey drift results (Figures 6-13) reveal consistent trends across NBC 105:2020 and IS 1893:2016, with the Nepali code prescribing markedly higher structural responses. Under the Equivalent Static Method (ESM), NBC 105:2020's Ultimate Limit State (ULS) conditions produced peak displacements of 74.045 mm (X-direction) and 75.393 mm (Y-direction)—exceeding IS 1893:2016 values (44.442 mm X, 50.07 mm Y) by 66.6% and 50.6%, respectively (Figures 6-7). Similarly, NBC 105:2020 ULS inter-storey drifts reached 0.004522 (X) and 0.005017 (Y), 67.3% and 64.2% higher than IS 1893:2016 maxima (0.002703 X, 0.003056 Y) (Figures 10-11). Overall, in the (ESM), the displacements under the Ultimate Limit State (ULS) for NBC 105: 2020 are the highest, while the Serviceability Limit State (SLS) values are somewhat lower but still greater than those for IS 1893 (Part 1): 2016. This divergence aligns with NBC 105:2020's amplified base shear coefficients and dual-state design philosophy, necessitating stricter displacement control measures.

The Response Spectrum Method (RSM) corroborated these findings, with NBC 105:2020 ULS displacements peaking at 72.586 mm (X) and 72.482 mm (Y)—106.7% and 107.6%

greater than IS 1893:2016's 35.112 mm (X) and 34.912 mm (Y) (Figures 8-9). Inter-storey drifts under RSM mirrored this pattern, with NBC 105:2020 maxima (0.00450 X, 0.004493 Y) exceeding IS 1893:2016 outputs (0.002159 X, 0.002154 Y) by 108.4% and 108.5%, respectively (Figures 12-13).

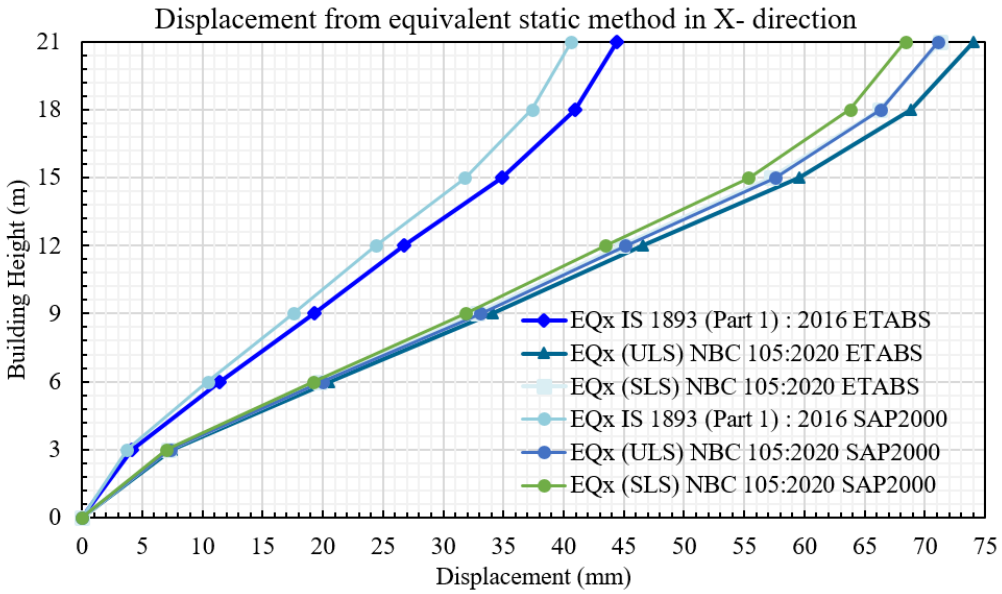

Figure 6. *Displacement from equivalent static method in X- direction.*

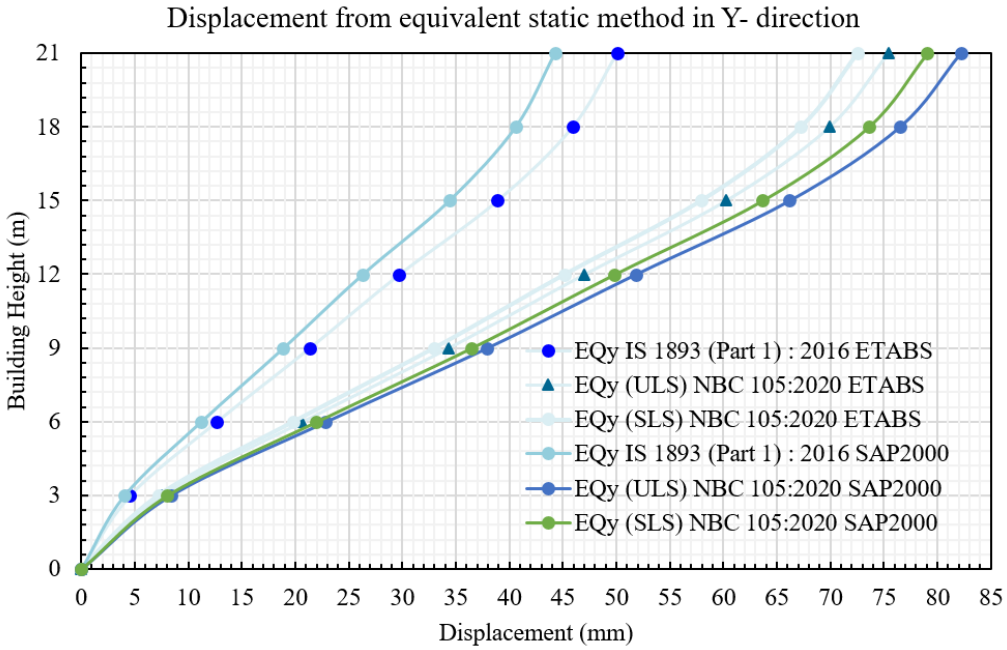

Figure 7. *Displacement from equivalent static method in Y- direction.*

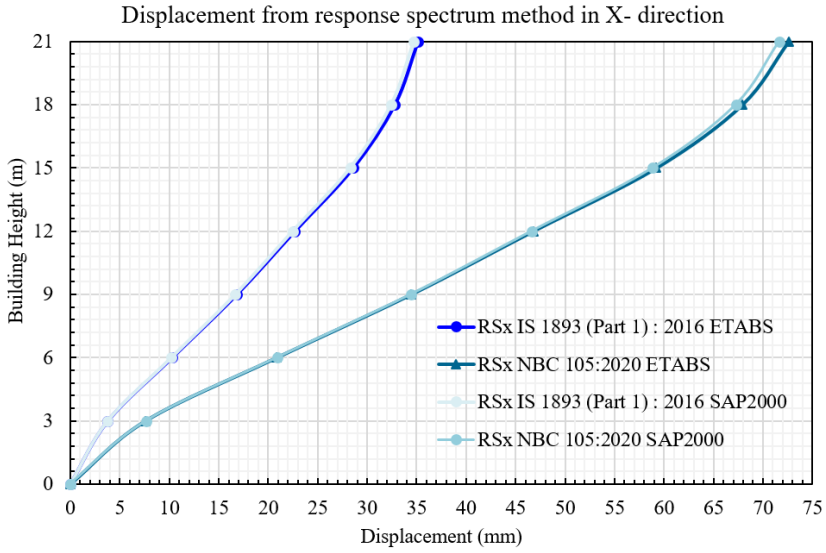

Figure 8. *Displacement from response spectrum method in X- direction.*

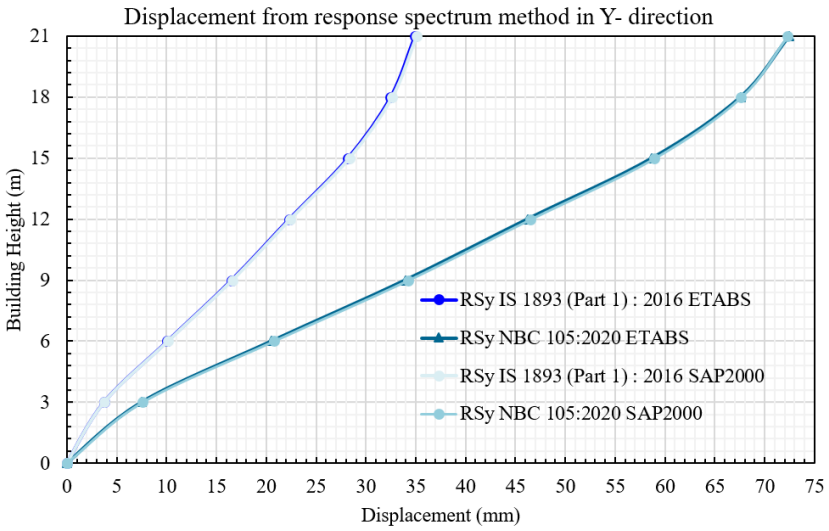

Figure 9. *Displacement from response spectrum method in Y- direction.*

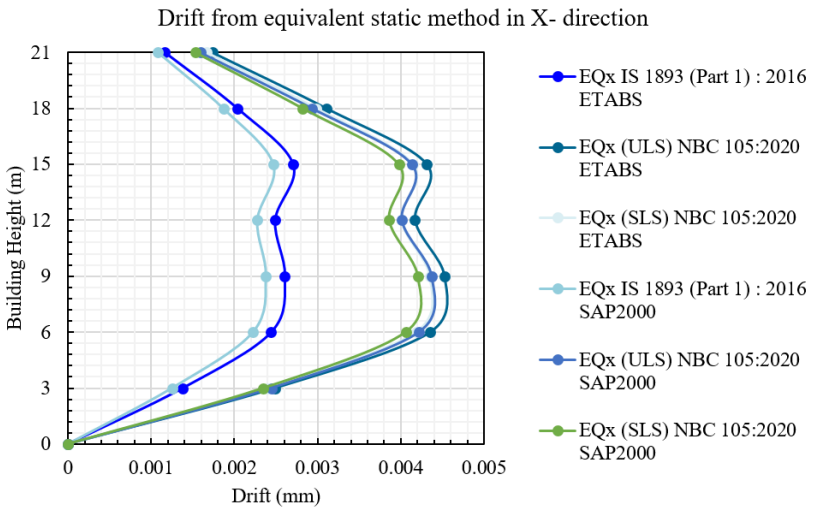

Figure 10. *Drift from equivalent static method in X- direction.*

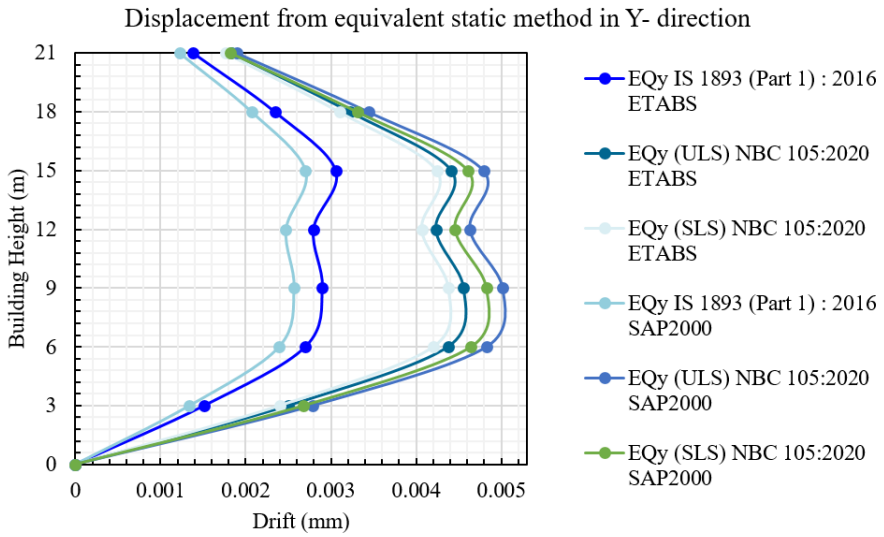

Figure 11. *Drift from equivalent static method in Y- direction.*

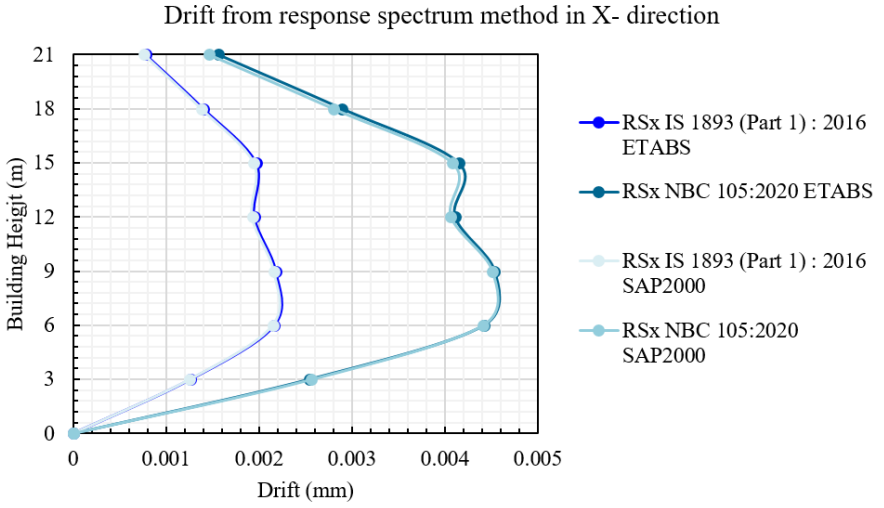

Figure 12. *Drift from response spectrum method in X- direction.*

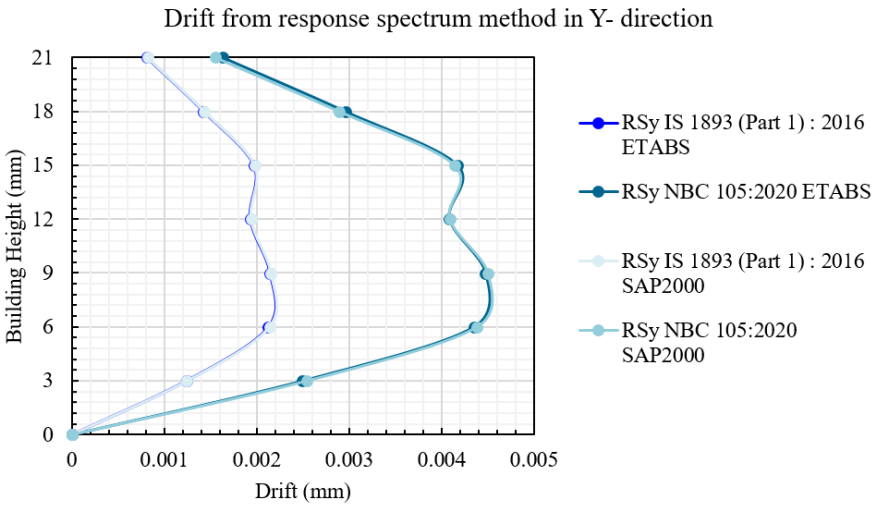

Figure 13. *Drift from response spectrum method in Y- direction.*

ETABS and SAP2000 exhibited consistent lateral displacement and drift patterns for both codes, with Response Spectrum Method (RSM) results showing nearly coinciding trends across software platforms. Notably, the magnitude of lateral displacement and drift was slightly higher under Equivalent Static Method (ESM) compared to RSM in both software.

6.3. Design Force and Reinforcement

Under actual loading conditions, columns must be designed as PMM (Axial Force and Biaxial Moment) elements to withstand the combined effects of axial loads (Pu) and bending moments (Mux, Muy). This approach ensures structural stability by enabling columns to resist bending stresses and maintain equilibrium under complex loading regimes [29]. Similarly, beams must resist concurrent shear forces (Vu) and bending moments (M) to ensure stability under transverse and flexural stresses. Critical to this framework is the stipulation in IS 456:2000 that torsion in beams must be evaluated in conjunction with shear rather than in isolation.

During concrete capacity checks in SAP2000 and ETABS under both codes, NBC 105:2020 flagged eight second-floor beams in ETABS for exceeding combined shear-torsion limits—a failure undetected in SAP2000—highlighting its rigorous compliance criteria. In contrast, IS 1893:2016 passed capacity checks in both software platforms. Design forces and reinforcement were derived exclusively from ETABS outputs, as SAP2000's member identification constraints complicate floor-wise data extraction. For beams, moments were analyzed at six locations (top/bottom at start/mid/end), with only the maximum value selected across all six points to represent critical bending demands. Similarly, shear and torsion were evaluated at three locations (start/mid/end), and only the maximum value from these points guided design in this paper. For columns, axial forces and biaxial moments were assessed at three locations (start/mid/end), with peak values selected to represent worst-case scenarios. In real-world construction using ETABS, beams are designed by analyzing all six points for flexure and three points for combined shear-torsion, whereas column design typically relies on data from a single critical point.

6.3.1. Design of Beam

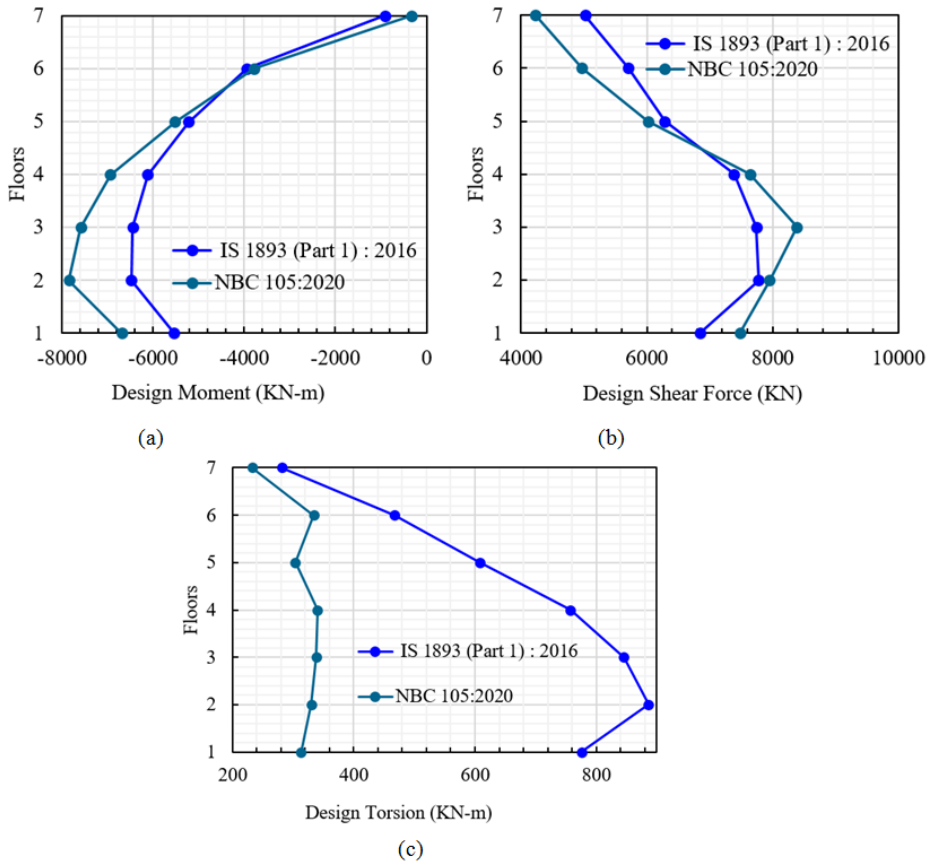

Figure 14. Beam design details floor-wise: (a) Design Moment (KN-m), (b) Design Shear Force (KN), (c) Design Torsion (KN-m).

It is evident from Figure 14-delineating floor-wise beam design details for (a) moments, (b) shear, and (c) torsion—that NBC 105:2020 prioritizes lower-floor robustness to address Nepal's high seismic risk. This prioritization arises from NBC's higher lateral forces compared to IS 1893 (Part 1):2016, which amplify moments in critical zones. The heightened moments (Figure 14a) result from NBC's dual stiffness modifiers (flexural and shear), which simulate post-cracking behavior more realistically and redistribute lateral loads to stiffer vertical members, concentrating demands on lower floors. This culminates in a 12% greater cumulative moment under NBC (−38,693 kN-m vs. −34,671 kN-m). The shifted shear distribution (Figure 14b), with elevated mid-to-lower floor values under NBC, reflects its conservative load combinations, though cumulative shear forces remain comparable (46,675 kN vs. 46,755 kN). Reduced torsion under NBC (Figure 14c) is evident across all floors, with a 110% lower cumulative torsion (2,191 kN-m vs. 4,621 kN-m).

Notably, IS 1893:2016 governs upper-floor moments and shear (Figure 14a-b), likely due to its reliance on flexural stiffness modifiers alone, which overestimates member stiffness and misrepresents load redistribution. This simpler modeling approach distributes forces more uniformly, leading to higher upper-floor demands. In contrast, NBC 105:2020's incorporation of shear stiffness modifiers and refined load combinations (Table 7) redistributes critical forces to lower floors, aligning with modern seismic codes emphasizing ductility and energy dissipation in vulnerable zones.

6.3.2. Design of Column

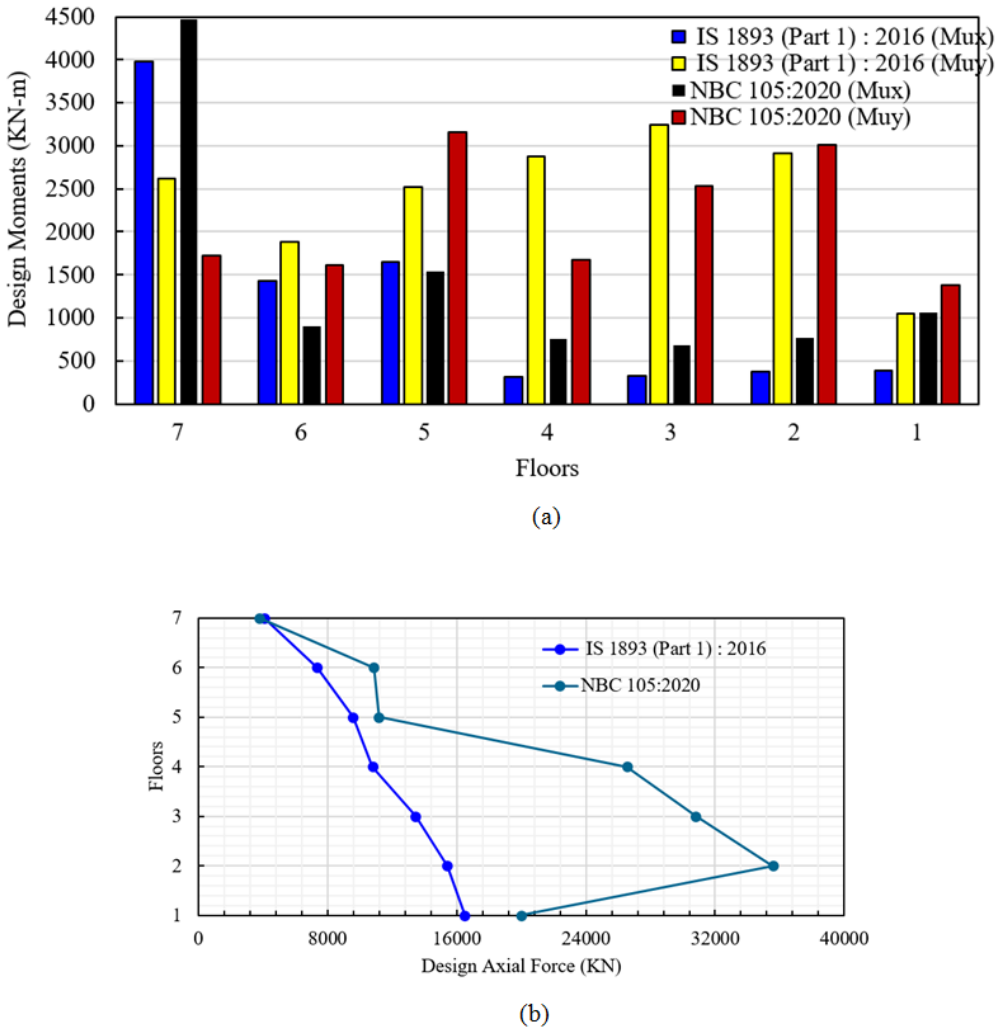

Figure 15. *Column design details floor-wise: (a) Design biaxial bending moments (KN-m), and (b) Axial forces (KN).*

The disparity in column design outcomes between NBC 105:2020 and IS 1893:2016 (Figure 15) arises from NBC's stringent seismic parameters, including nearly double the base shear and higher lateral displacements, which amplify de-

mands on critical structural members. Combined with NBC's dual stiffness modifiers (Table 6)—reducing beam stiffness relative to columns—these provisions redistribute lateral and gravity loads to stiffer vertical members, magnifying axial forces (79% cumulative increase: 138,668 kN vs. 77,122 kN), particularly in lower floors, with a 146% increase in the 4th floor, 129% in the 3rd, 130% in the 2nd, and 21% in the 1st floor (Figure 15b). In parallel, directional bending moments (Figure 15a) diverge significantly: NBC 105:2020 prioritizes higher X-direction moments (Mux) in lower floors. This contrast extends to their underlying philosophies: NBC's explicit modeling of stiffness degradation and directional load prioritization enhances ductility in critical zones, while IS 1893:2016's conservative stiffness assumptions distribute forces uniformly, resulting in lighter axial demands and less directionally optimized moments. NBC's elevated base shear thresholds and rigorous load redistribution mechanics underscore its alignment with Nepal's high seismic risk, balancing safety and pragmatism through advanced seismic resilience strategies. IS 1893:2016, by contrast, reflects a generalized methodology suited for broader applications but less tailored to localized seismic intensity.

6.3.3. Reinforcement in Beams and Columns

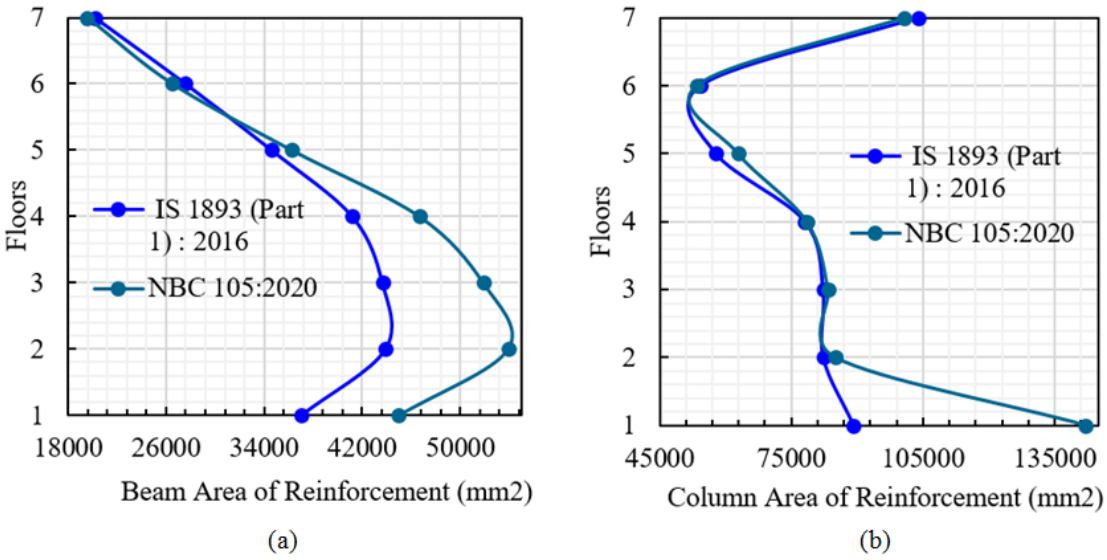

Figure 16. *Floor-wise reinforcement area distribution: (a) Beam reinforcement area (mm²), (b) Column reinforcement area (mm²).*

Figure 16(a–b) delineates floor-wise reinforcement distributions, revealing NBC 105:2020's 12.7% higher cumulative beam reinforcement (279,709 mm ²vs. 248,222 mm ³) and 10.6% greater column reinforcement (605,995 mm² vs. 547,948 mm²) compared to IS 1893:2016. Columns under NBC 105:2020 show pronounced reinforcement spikes at critical lower floors (e.g., 130% increase at Floor 2), driven by its dual stiffness modifiers and doubled base shear, which amplify axial and moment demands through realistic post-cracking stiffness degradation. Contrary to [14], which reported IS 1893:2016 requires more reinforcement than the NBC 105:2020 in bare-frame models under dead load of structure only, this study demonstrates NBC 105:2020's stricter updated provisions (stiffness modifiers and seismic load criteria) reverse this trend, yielding significant steel escalation over IS 1893 (part 1):2016. This contrasts with [12]'s claim of negligible differences under NBC 105:2019, highlighting the critical impact of the 2020 revision. While [13] observed overall in the whole structure 4.39% steel increase using NBC 105:2020 without property modifiers, this study's incorporation of stiffness modifiers amplifies the difference, underscoring NBC 105:2020's emphasis on robust column designs to mitigate seismic risks. These findings align with ductility-focused global practices but necessitate higher construction costs due to stricter code requirements.

7. Conclusion

This study rigorously evaluates the seismic parameters, design forces and reinforcement demands of major structural elements: beams and columns, disparities between Nepal's NBC 105:2020 and India's IS 1893:2016 for regular reinforced concrete structures, leveraging finite element modeling (ETABS and SAP2000). While both software platforms were employed for seismic analysis to predict structural behavior, ETABS was exclusively used for member design and reinforcement calculation due to its user-friendly output generation floor wise. A concrete design check—verification of structural members against code-based strength and detailing requirements—revealed critical shear-torsion failures in eight

second-floor beams in ETABS under NBC 105:2020, undetected by SAP2000, underscoring its precision in safety, while IS 1893:2016 passed this checks in both software platforms.

Compared to IS 1893 (part 1):2016, NBC 105:2020 mandates nearly double the base shear, reflecting Nepal's heightened seismic risk, and amplifies structural demands: lateral displacements surged by 66.6% (X) and 50.6% (Y) under the Equivalent Static Method (inter-storey drifts: 64.2–67.2%) and by 106% (X) and 107% (Y) under the Response Spectrum Method (drifts: 108.4–108.5%). While in this case study absolute magnitudes of displacements and drifts were slightly higher in Equivalent Static analyses, both ETABS and SAP2000 exhibited strong consistency in lateral displacement and drift patterns under both static and dynamic analysis; however, dynamic analysis demonstrated nearly identical trends across codes, validating the reliability of Response Spectrum results for seismic assessments.

Floor-wise analysis revealed NBC 105:2020's distinct impact on member design compared to IS 1893:2016. For beams, NBC 105:2020 increased design moments by 11.6% and reduced torsion by 110%, necessitating 12.7% more reinforcement—particularly in lower floors—while shear forces remained comparable. For columns, NBC 105:2020 induced floor-wise fluctuations in biaxial moments: 20.25% higher X-direction moments but 11.81% lower Y-direction moments versus IS 1893:2016, alongside a dramatic 79.78% surge in axial forces. Column reinforcement under NBC 105:2020 rose by 10.6% compared to IS 1893:2016, peaking at 130% in lower floors, driven by its conservative stiffness modifiers that prioritize column robustness over beam flexibility, redistributing loads to vertical members. The code's emphasis on lower-floor axial load concentration and moment redistribution underscores its seismic resilience strategy.

The conclusion made here does not represent a broad perspective, as only a single RC building was used in this case study. However, it is clear that the increased base shear, design forces, reinforcement and load redistributions directly affects the construction cost making design more expensive under NBC 105:2020 than IS 1893 (Part 1): 2016. While stricter seismic standard ensures safer construction, it comes with higher financial burden. The study suggests that municipalities and engineers in Nepal to adopt NBC 105:2020 for better seismic safety because of it's complex geology and high seismic vulnerability.

Abbreviations

ESM	Equivalent Static Method
RSM	Response Spectrum Method
EQx (ULS)	Equivalent Static Method Loading in the x-direction for Ultimate Limit State
EQy (ULS)	Equivalent Static Method Loading in the y-direction for Ultimate Limit State
EQx (SLS)	Equivalent Static Method Loading in the x-direction for Serviceability Limit State
EQy (SLS)	Equivalent Static Method Loading in the y-direction for Serviceability Limit State
RSx	Response Spectrum Method Loading in the x-direction
RSy	Response Spectrum Method Loading in the y-direction

Funding

This research did not receive any specific grant from public, commercial, or not-for-profit funding agencies.

Data Availability Statement

The data that support the findings of this study are available from the corresponding author upon reasonable request.

Conflicts of Interest

The authors declare no conflicts of interest.

References

[1] Center for Excellence in Disaster Management and Humanitarian Assistance (2015). Nepal disaster management reference handbook. Available at: https://www.cfe-dmha.org/LinkClick.aspx?fileticket=xEUbtKHdfR4%3D&portalid=0 [Accessed 15 October 2015].

[2] Dhital, M. R., & Adhikari, B. R. (2020). Thrust sheets, tectonic windows, and intermontane basins in the Nepal Himalaya. Structural Geometry of Mobile Belts of the Indian Subcontinent, 233-254. https://doi.org/10.1007/978-3-030-40593-9_11

[3] Bilham, R., & Ambraseys, N. (2005). Apparent Himalayan slip deficit from the summation of seismic moments for Himalayan earthquakes, 1500–2000. Current Science, 89(10), 1658-1663. Available at: http://www.jstor.org/stable/24110492

[4] Das, S., Gupta, I. D., & Gupta, V. K. (2006). A probabilistic seismic hazard analysis of Northeast India. Earthquake Spectra, 22(1), 1-27. https://doi.org/10.1193/1.2163914

[5] Chaulagain, H., Gautam, D., & Rodrigues, H. (2018). Revisiting major historical earthquakes in Nepal: Overview of 1833, 1934, 1980, 1988, 2011, and 2015 seismic events. Impacts and Insights of the Gorkha Earthquake, 1-17. https://doi.org/10.1016/B978-0-12-812808-4.00001-8

[6] Adhikari, L. B., Laporte, M., Bollinger, L., Vergne, J., Lambotte, S., Koirala, B. P.,... & Perrier, F. (2023). Seismically active structures of the Main Himalayan Thrust revealed before, during and after the 2015 Mw 7.9 Gorkha earthquake in Nepal. Geophysical Journal International, 232(1), 451-471. https://doi.org/10.1093/gji/ggac281

[7] Goda, K., Kiyota, T., Pokhrel, R. M., Chiaro, G., Katagiri, T., Sharma, K., & Wilkinson, S. (2015). The 2015 Gorkha Nepal earthquake: insights from earthquake damage survey. Frontiers in Built Environment, 1, 8. https://doi.org/10.3389/fbuil.2015.00008

[8] Guragain, R., Pradhan, S., Maharjan, D. K., & Shrestha, S. N. (2018). Building code implementation in Nepal: An experience on institutionalizing disaster risk reduction in local governance system. Science and Technology in Disaster Risk Reduction in Asia, 207-220. https://doi.org/10.1016/B978-0-12-812711-7.00013-4

[9] Malla, S., Alagirisamy, M., Dangol, P., & Giri, O. P. (2024). Comparative analysis of an apartment building using seismic codes NBC 105: 1994 and NBC 105: 2020 (A case study). Engineering, Technology & Applied Science Research, 14(4), 15916-15922. https://doi.org/10.48084/etasr.7858

[10] Lizundia, B., Shrestha, S. N., Bevington, J., Davidson, R., Jaiswal, K., Jimee, G. K., & Ortiz, M. (2016). M7.8 Gorkha, Nepal earthquake on April 25, 2015 and its aftershocks. EERI Earthquake Reconnaissance Team Report, 1-185.

[11] Banjara, R., Thapa, D., Katuwal, T. B., & Adhikari, S. (2021). Seismic Behaviour of Buildings as per NBC 105: 1994, NBC 105: 2020 and IS 1893: 2016. In *IOE Graduate Conference* (pp. 1461-1471).

[12] Bhusal, B., & Paudel, S. (2021). Comparative study of existing and revised codal provisions adopted in Nepal for analysis and design of Reinforced concrete structure. *Int J Adv Eng Manag*, *6*, 25-42.

[13] Pokhrel, M., Adhikari, U., Dhakal, S., Dhakal, A., Ghimire, S., & Shrestha, A. (2023). Comparative Seismic Analysis, Design, and Cost Estimation of a Residential Building. *International Journal on Engineering Technology*, *1*(1), 27-36.

[14] Sapkota, A., Sapkota, B., Poudel, J., & Giri, S. (2024). Comparative study on the seismic performance of a typical low-rise building in Nepal using different seismic codes. *Asian Journal of Civil Engineering*, *25*(6), 4373-4394. https://doi.org/10.1007/s42107-024-01053-5

[15] Syed, E. U., & Manzoor, K. M. (2022). Analysis and design of buildings using Revit and ETABS software. Materials Today: Proceedings, 65, 1478-1485. https://doi.org/10.1016/j.matpr.2022.04.463

[16] Bureau of Indian Standards (2000). IS 456:2000 Plain and Reinforced Concrete - Code of Practice New Delhi: BIS.

[17] NBC 105:2020. National Building Code of Nepal, Seismic Design of Buildings in Nepal.

[18] Bureau of Indian Standards 2016 Indian Standard Code (IS 1893). Part I: Criteria for earthquake resistant design of structures: General provisions and buildings.

[19] Wiyono, D. R., Milyardi, R., & Lesmana, C. (2018). The effect of shear wall configuration on seismic performance in the hotel building. MATEC Web of Conferences, 159, 02074. https://doi.org/10.1051/matecconf/201815902074

[20] Tanuwidjaja, H. R., Santoso, G. K., & Tanuwidjaja, E. (2021). Rigidity boundaries of floor reinforced concrete diaphragm. In Proceedings of the 6th International Conference on Civil, Offshore and Environmental Engineering (ICCOEE2020) (pp. 476-483). Springer, Singapore. https://doi.org/10.1007/978-981-33-6311-3_55

[21] Liu, W. B., Gheni, M., & Yu, L. (2011). Effect of mesh size of finite element analysis in modal analysis for periodic symmetric struts support. Key Engineering Materials, 462, 1008-1012. http://dx.doi.org/10.4028/www.scientific.net/KEM.462-463.1008

[22] Sharma, P., & Gupta, T. (2022). Comparative investigation on mode shapes and natural frequency of low-rise RC frame building. In Advances in Construction Materials and Sustainable Environment: Select Proceedings of ICCME 2020 (pp. 885-898). Springer, Singapore. https://doi.org/10.1007/978-981-16-6557-8_72

[23] Maskey, P. N., Tamrakar, M. R., Bista, M. K., Ojha, S., Gautam, B. K., Acharya, I., & Dhakal, R. (2020). NBC105: 2019 Seismic design of buildings in Nepal: New provisions in the code.

[24] Pitilakis, K., Anastasiadis, A., Pitilakis, D., Trevlopoulos, K., & Senetakis, K. (2010). Elastic demand spectra. In Advances in Performance-Based Earthquake Engineering (pp. 89-99). Springer. https://doi.org/10.1007/978-90-481-8746-1_9

[25] Aninthaneni, P. K., & Dhakal, R. P. (2016). Prediction of fundamental period of regular frame buildings. Bulletin of the New Zealand Society for Earthquake Engineering, 49(2), 175-189. https://doi.org/10.5459/bnzsee.49.2.175-189

[26] Ramos, F. B. M. (2023). Seismic response of reinforced concrete buildings, considering the effective stiffness in beams, columns, and structural walls. South Florida Journal of Development, 4(10), 3981-3994. https://doi.org/10.46932/sfjdv4n10-020

[27] Scanlon, A., & Bischoff, P. H. (2008). Shrinkage restraint and loading history effects on deflections of flexural members. ACI Structural Journal, 105(4), 498. https://doi.org/10.14359/19864

[28] Tang, T. O., & Su, R. K. L. (2014). Shear and flexural stiffnesses of reinforced concrete shear walls subjected to cyclic loading. The Open Construction & Building Technology Journal, 8(1). http://dx.doi.org/10.2174/1874836801408010104

[29] Bouzid, T., & Demagh, K. (2011). Practical method for analysis and design of slender reinforced concrete columns subjected to biaxial bending and axial loads. Slovak Journal of Civil Engineering, 19(1), 24-32. https://doi.org/10.2478/v10189-011-0004-1